



OPEN

A pilot study of 3D tissue-engineered bone marrow culture as a tool to predict patient response to therapy in multiple myeloma

Kinan Alhallak^{1,2,7}, Amanda Jeske^{1,2,3,7}, Pilar de la Puente^{3,4,7}, Jennifer Sun^{1,2}, Mark Fiala⁵, Feda Azab³, Barbara Muz¹, Ilyas Sahin⁶, Ravi Vij⁵, John F. DiPersio⁵ & Abdel Kareem Azab^{1,2,3}✉

Cancer patients undergo detrimental toxicities and ineffective treatments especially in the relapsed setting, due to failed treatment attempts. The development of a tool that predicts the clinical response of individual patients to therapy is greatly desired. We have developed a novel patient-derived 3D tissue engineered bone marrow (3DTEBM) technology that closely recapitulate the pathophysiological conditions in the bone marrow and allows *ex vivo* proliferation of tumor cells of hematologic malignancies. In this study, we used the 3DTEBM to predict the clinical response of individual multiple myeloma (MM) patients to different therapeutic regimens. We found that while no correlation was observed between *in vitro* efficacy in classic 2D culture systems of drugs used for MM with their clinical efficacious concentration, the efficacious concentration in the 3DTEBM were directly correlated. Furthermore, the 3DTEBM model retrospectively predicted the clinical response to different treatment regimens in 89% of the MM patient cohort. These results demonstrated that the 3DTEBM is a feasible platform which can predict MM clinical responses with high accuracy and within a clinically actionable time frame. Utilization of this technology to predict drug efficacy and the likelihood of treatment failure could significantly improve patient care and treatment in many ways, particularly in the relapsed and refractory setting. Future studies are needed to validate the 3DTEBM model as a tool for predicting clinical efficacy.

Personalized medicine is the use of the patient's own tumor genotype and/or phenotype to create the most appropriate therapeutic choice for individual patients. While precision cancer medicine studies have mainly focused on genomics, most patients with cancer who receive genomic testing have limited benefit from this strategy¹. This is due to the fact that drug sensitivity and resistance depend not only on genomics, but also on epigenetic factors, and most importantly the interactions with tumor microenvironment (TME)². 2D classic tissue culture models lack significant biological features of the TME such as oxygen gradients (tumor hypoxia) and drug gradients, which have critical effect on the sensitivity of cancer cells to therapy in different hematologic malignancies such multiple myeloma (MM)³, leukemia⁴, and lymphoma^{5,6}. While synthetic 3D models such as polymeric matrices exhibit advantages compared to classic 2D cultures, they utilize non-physiological materials that may change the biological properties of the tumor cells⁷. In addition, the presence of accessory cells found in the TME, aside from the tumor cells, was shown to play a critical role in the TME-induced resistance^{2,8}. Therefore, a

¹Department of Radiation Oncology, Washington University School of Medicine, 4511 Forest Park Ave, St. Louis, MO 63108, USA. ²Department of Biomedical Engineering, Washington University, St. Louis, MO, USA. ³Cellatrix LLC, St. Louis, MO, USA. ⁴Cancer Biology and Immunotherapies Group, Sanford Research, Sioux Falls, SD, USA. ⁵Department of Medicine, Washington University School of Medicine, St. Louis, MO, USA. ⁶Division of Hematology/Oncology, The Warren Alpert Medical School, Brown University, Providence, RI, USA. ⁷These authors contributed equally: Kinan Alhallak, Amanda Jeske and Pilar de la Puente. ✉email: kareem.azab@wustl.edu

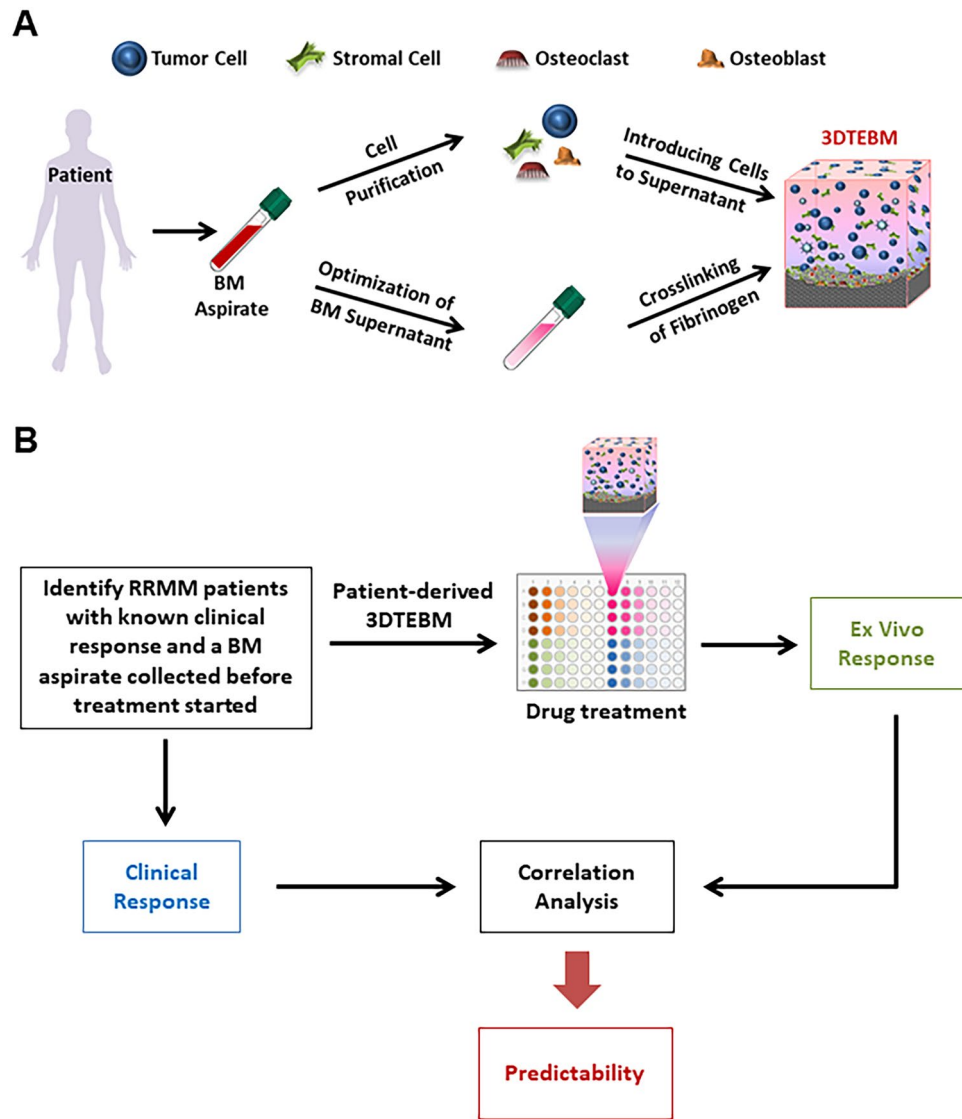


Figure 1. Novel patient-derived 3D Tissue-Engineered Bone Marrow (3DTEBM) used to predict clinical efficacy in individual cancer patients for personalized medicine. **(A)** The 3DTEBM includes all the accessory and primary cancer cells found in the bone marrow (BM), as well as growth factors, enzymes, and cytokines naturally found in the TME which better recapitulates the BM niche found in patients. **(B)** Clinical workflow for a retrospective study testing 3DTEBM predictability for multiple myeloma (MM) patient clinical response.

patient-derived 3D model of primary tumor cells, including other accessory cells, without exogenous polymers, that truly recapitulates the TME is warranted.

We have previously created a patient-derived 3D tissue-engineered bone marrow (3DTEBM) culture model, which is predominantly derived from BM aspirates of patients with hematologic malignancies (Fig. 1A). It utilizes autologous BM supernatant to create the 3D matrix, in which we incorporate primary cancer cells, along with all the other accessory cells in the BM microenvironment, without the addition of exogenous materials⁹. The BM cellular and non-cellular constituents recapitulate the malignant TME enabling primary cells progression *ex vivo*⁹. In addition, the hydrogel-like 3D structure derived from the crosslinking of endogenous fibrinogen results in a “soft” culture compared to other synthetic polymers, which better recapitulates the BM tissue^{2,10}. Moreover, the 3D structure recreated oxygen gradients, resembling tumor hypoxic BM niche. It was demonstrated that the 3DTEBM was able to promote biological effects which were not demonstrated in regular 2D culture^{2,10–12}, and allow the survival and proliferation of freshly isolated or frozen primary cancer cells *ex vivo*, in both MM^{10,12} and leukemia¹¹.

The 3DTEBM model was shown to mimic the malignant BM condition in several hematologic malignancies including MM⁹, acute myeloid leukemia, chronic myeloid leukemia, and chronic lymphocytic leukemia¹¹, allowing primary cell progression *ex vivo* and better representation of drug resistance/sensitivity^{7,9,11}. Therefore, the

MM drug	Literature C _{ss} (nM)		2D Literature IC ₅₀ (nM)	
Carfilzomib	5	^{16–18}	5.3	^{19–21}
Bortezomib	10	²²	5	^{19,23–25}
Ixazomib	15	^{26,27}	15.8	^{24,28}
Panobinostat	10	^{29,30}	31.2	^{31,32}
Lenalidomide	1000	^{33,34}	600	^{35–37}
Pomalidomide	130	³⁸	14,773.7	^{39,40}
Dexamethasone	500	⁴¹	11,900.7	^{42–45}
Etoposide	30,000	^{46,47}	28,000.1	^{48–50}
Doxorubicin	3000	⁵¹	14,536.8	^{52–54}
Melphalan	2000	^{55,56}	10,000	^{57–59}

Table 1. Names, concentrations, and literature for each of the drugs used.

3DTEBM arises as a unique model for ex vivo drug screening and predictive tool to determine clinical efficacy in individual cancer patients for personalized medicine.

MM is the cancer of plasma cells within the BM and represents the second most common hematologic malignancy¹³. Although therapeutic options have significantly broadened over the years, the disease is challenged by frequent relapses. Relapsed/refractory MM (RRMM) often becomes non-responsive to previous lines of treatment and has significantly poorer survival outcome¹⁴. Physicians are faced with a difficult task to choose a right treatment regimen for RRMM patients¹⁵. In this study, we aimed to conduct a retrospective study that tests the ability of the ex vivo 3DTEBM platform to predict the clinical response in individual MM patients, to help decision-making process for RRMM. 3DTEBM cultures were developed for each patient from BM biopsies obtained before the start of clinical treatment. Cultures were treated ex vivo with the same treatment regimen each patient received clinically. Finally, ex vivo responses in the 3DTEBM were correlated to clinical responses, to test overall predictability (Fig. 1B). We hypothesized that the 3DTEBM will be able to predict clinical responses of RRMM patients.

Results

Despite the ability of therapeutic agents to eradicate MM in vitro in classic 2D culture models, there is often little correlation with clinical activity in patients. To demonstrate this discrepancy between drug efficacy in laboratory settings and clinical outcomes, we compared the in vitro efficacious concentration to the clinical efficacious concentrations of 10 drugs used for the treatment of MM (Table 1). We defined the efficacious clinical concentration as the steady state plasma drug concentration (C_{ss}) reached after administration of clinically effective doses. We performed a literature search and determined C_{ss} values based on pharmacokinetic data from Phase 1 and/or Phase 2 clinical trials (Table 1). Next, we defined the efficacious in vitro concentration as the half-inhibitory concentration (IC₅₀) at 48 h for each drug in MM cell lines. The IC₅₀ values for the 2D classic tissue culture system was determined by both literature search and experimental study. With these information, we calculated the correlation between the 2D IC₅₀ values and clinical C_{ss} values. We found that there was no correlation between the in vitro 2D IC₅₀ and the clinical C_{ss} values, represented by a correlation coefficient of R² = 0.601 for literature studies (Fig. 2A) and R² = 0.019 for experimental study (Fig. 2B).

We then determine the IC₅₀ values of the same drugs in the 3DTEBM culture system, and their correlation with clinical C_{ss} values. MM cells lines were cultured within the 3DTEBM in combination with MM patient BM microenvironment, and the MM cell survival was determined at 48 h (Fig. 2C). In contrast to 2D tissue cultures, we found that the IC₅₀ values in the 3DTEBM directly correlated with the clinical C_{ss}, represented by a correlation coefficient of R² = 0.993 (Fig. 2D). The individual drug's dose response curves are also shown (Fig. 2E and Supp Fig. 1).

Next, we conducted a retrospective clinical trial to determine if the 3DTEBM platform is able to predict each patient's clinical response by recreating the same treatment regimen ex vivo. 19 RRMM patients with known clinical responsiveness to the regimen they received were identified. The patients had a mix of responsiveness: patients with partial response (PR), very good partial response (VGPR) and/or complete remission (CR) were categorized as "responsive", while patients with stable disease and/or progressive disease (PD) were categorized as "non-responsive". Patient demographics for the primary MM samples used are shown in Table 2.

We developed 3DTEBM cultures using individual patient's BM samples collected prior to the start of their prescribed treatment regimen. Samples were treated for 4 days with the respective regimen at increasing concentrations, and primary cell survival was determined as % of untreated (Fig. 3A). The ex vivo response was given back to the clinical teams as "responsive" or "non-responsive". To demonstrate the range of ex vivo response we observe in the 3DTEBM, primary cell survival curves resulting from 3DTEBM cultures derived from two MM patients are presented (Fig. 3B), each of which were treated with the same drug regimen. MM Patient 4 did not respond (p-value of 0.9642) to the combination treatment of bortezomib and dexamethasone, while MM Patient 4 responded to the treatment (p-value of 0.0001). Additionally, survival curves for all 19 patients representing their ex vivo response are shown in Supplemental Fig. 2. The clinical teams correlated the ex vivo response for each patient with the clinical response.

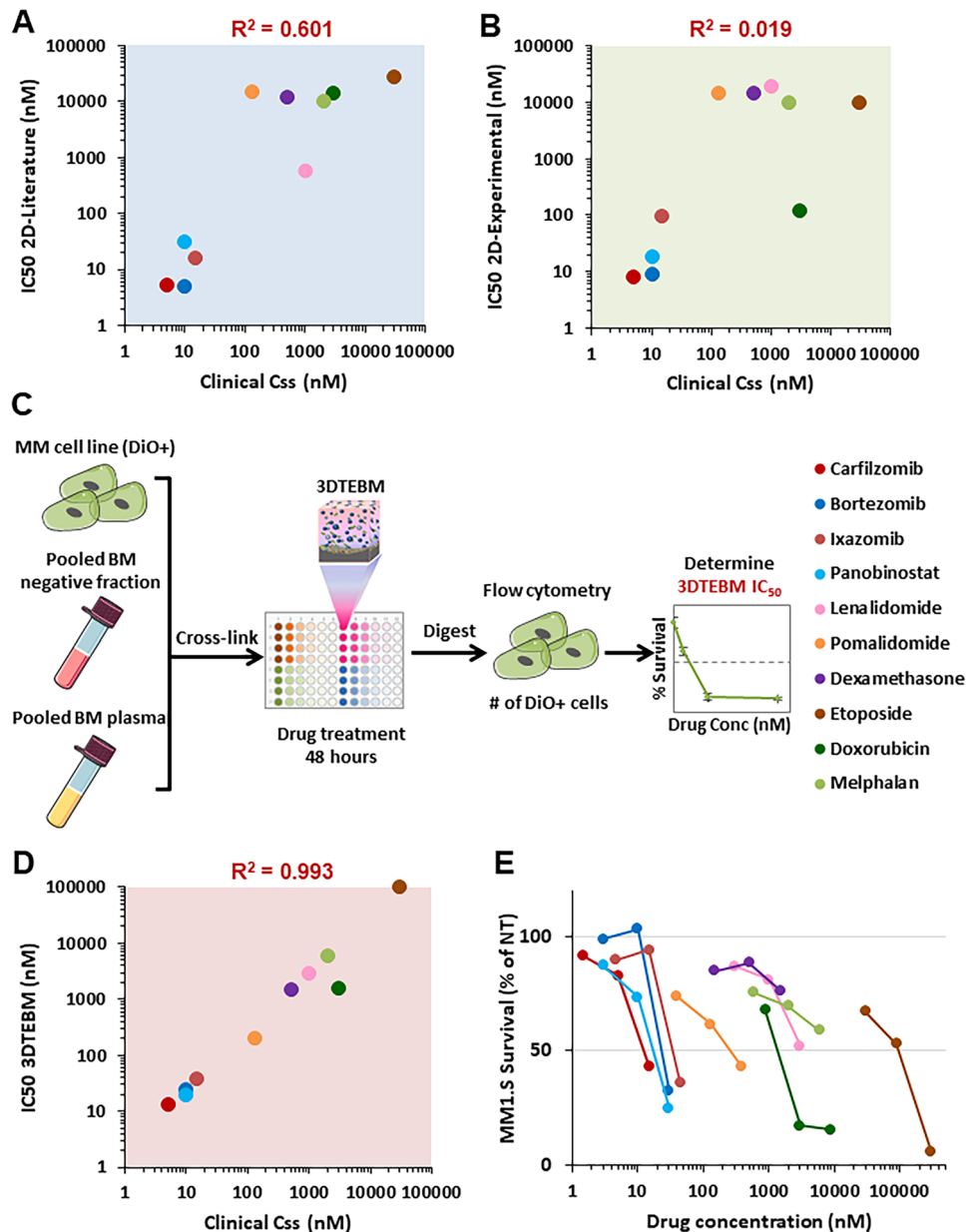


Figure 2. The 3DTEBM efficaciously correlates between half maximal inhibitory concentration (IC₅₀) and clinical steady state plasma concentration (C₅₀) values of MM drugs. IC₅₀ values determined by (A) 2D literature research and (B) 2D experimental studies both correlated poorly with clinical C₅₀ values. (C) Schematic of experimental procedure for determining 3DTEBM IC₅₀ in cell lines. (D) IC₅₀ values determined by 3DTEBM correlated well with clinical C₅₀ values. (E) 3DTEBM dose response curves for all 10 drugs tested in MM1.S cells. Correlation coefficients (R^2) were calculated from linear regression fitting.

Finally, we developed a summary, highlighting the predictability of patient response by the 3DTEBM ex vivo, based on the drug regimen that the patient received clinically. The 3DTEBM model was able to predict the response in 89% of the MM patient cohort (Fig. 3C). Particularly, it was able to predict 100% of the non-responsive cases in MM, and 75% in MM responsive cases. A more detailed description of the clinical responses, and responses predicted by 3DTEBM for each patient sample are listed in Table 3.

Discussion

The majority of clinical trial failures are due to a lack of drug efficacy (52%)⁶⁰. The traditional 2D culture system does not recapitulate the TME nor the clinical outcomes. In this study, we demonstrated that there was no correlation between the in vitro IC₅₀ values in classic 2D culture systems and the clinically efficacious concentrations. These findings could partially explain the discrepancies between drug efficacy in laboratory settings and the unsatisfactory clinical outcomes in hematologic malignancies. In contrast, IC₅₀ values obtained in the

Clinical characteristics	All patients (n = 19)
Median Age	61.8 years (range 46–82)
Gender	Value (%)
Male	7 (37)
Female	12 (63)
Race	Value (%)
African American	2 (11)
White	17 (89)
Treatment Status	Value (%)
Relapse/Progression	19 (100)

Table 2. Clinical characteristics of patients with multiple myeloma.

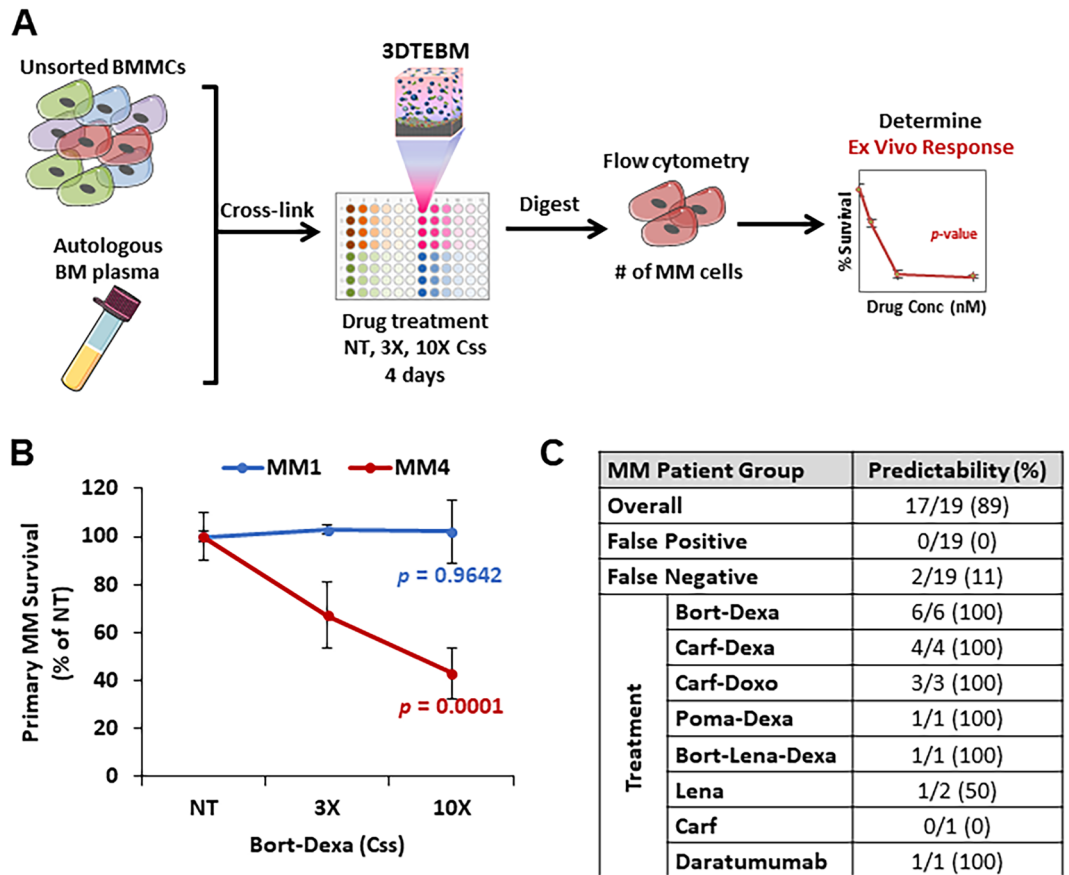


Figure 3. Retrospective predictability for MM patient cohort. (A) Schematic of experimental procedure for determining ex vivo response in 3DTEBM utilizing patient unsorted bone marrow mononuclear cells (BMMCs) and autologous BM plasma. (B) Example primary MM cell survival for a responsive and a non-responsive MM patient sample. Statistical significance is analyzed by single-factor ANOVA; responsive if $p < 0.05$. (C) Overall predictability of patient clinical response for each drug therapy using the 3DTEBM platform.

3DTEBM showed direct correlation with clinically efficacious concentrations. This suggests that, unlike regular culture systems, the 3DTEBM platform provides a pathophysiologically relevant model that could be used for drug development and help predict drug efficacy in individual patients.

Recent studies in the field have suggested a variety of ex vivo approaches to identify drugs with clinical efficacy in hematologic malignancies^{61–64}. Despite intensive efforts in the field, reliable, cost-effective and simple ex vivo model that is applicable in the clinical practice for drug efficacy prediction is still lacking⁶². A reliable method predicting drug efficacy and the likelihood of treatment failure could significantly improve patient care and treatment in many ways particularly in relapsed/refractory setting. Potential benefits will include but not limited to avoiding the toxicity and reducing the costs of therapies that prove to be ineffective.

Patient	Treatment	3DTEBM		Clinical Response	Predictive
		P-value	Response		
1	Bort-Dexa	0.9642	Not sensitive	PD	Yes
2	Bort-Dexa	<0.0001	Sensitive	PR	Yes
3	Bort-Dexa	0.4629	Not sensitive	PD	Yes
4	Bort-Dexa	0.0001	Sensitive	PR	Yes
5	Bort-Dexa	<0.0001	Sensitive	PR	Yes
6	Bort-Dexa	0.3522	Not sensitive	PD	Yes
7	Carf-Dexa	0.0008	Sensitive	VGPR	Yes
8	Carf-Dexa	0.7661	Not sensitive	PD	Yes
9	Carf-Dexa	0.1092	Not sensitive	PD	Yes
10	Carf-Dexa	0.4130	Not sensitive	PD	Yes
11	Carf-Doxo	0.0038	Sensitive	PR	Yes
12	Carf-Doxo	0.1006	Not sensitive	PD	Yes
13	Carf-Doxo	0.5779	Not sensitive	PD	Yes
14	Bort-Lena-Dexa	0.5334	Not sensitive	PD	Yes
15	Lena	0.3361	Not sensitive	PR	No
16	Lena	0.0236	Sensitive	VGPR	Yes
17	Carf	0.1405	Not sensitive	CR	No
18	Poma-Dexa	0.6661	Not sensitive	PD	Yes
19	Daratumumab	0.5263	Not sensitive	PD	Yes

Table 3. Clinical responses and predictability of 3DTEBM.

In this retrospective study, we demonstrated that the 3DTEBM technology was able to predict clinical therapeutic response with 89% accuracy. These results suggest the 3DTEBM as a feasible platform for predicting therapeutic responses in MM with a high predictive accuracy within a clinically actionable time frame. Routine bone marrow biopsy, in addition to its diagnostic value, can be now utilized in the 3DTEBM as a treatment decision-making tool. Such platforms can provide precise clinical insight about the efficacy of different treatment plans in a timely manner (less than a week), and assist physicians to propose the best choice of therapy for their individual patients.

3DTEBM is emerging as a promising personalized medicine platform for prediction of clinical responses to therapy in individual RRMM patients, not only because of its ability to allow proliferation of patient-derived primary tumor cells and its ability to mimic patient's own pathophysiologic BM TME *ex vivo*, but also because of its accuracy, reproducibility, short turnaround time, high-throughput potential, and low-cost. Future prospective studies are needed to validate these significant findings by expanding clinical sample size, and testing the ability of the 3DTEBM to prospectively predict effective treatment for improved response in hematologic malignancies.

Methods

Materials and reagents. Lipophilic cell tracer (DiO) was purchased from Invitrogen (Eugene, OR). All antibodies used for flow cytometry were purchased from BD Biosciences (San Jose, CA) unless otherwise noted. Red Blood Cell (RBC) lysis buffer was purchased from Biolegend (San Diego, CA). All chemicals were purchased from Millipore Sigma (Burlington, MA). All drugs were purchased from Selleck Chemicals (Houston, TX), except Daratumumab (Janssen, Beerse, Belgium), which was generously provided to us by the pharmacy at Washington University. MM cell lines were obtained from American Type Culture Collection (Manassas, Virginia).

Patient primary BM samples. MM pre-treated patient samples were collected under informed consent, in concordance with the Institutional Review Boards (IRBs) of Washington University in St. Louis School of Medicine (IRB protocol number 201102270). All studies were in accordance with the Declaration of Helsinki. Plasma was isolated by centrifugation, and BM mononuclear cells (BMMCs) were isolated by RBC lysis, as described before⁶⁵. To acquire BM negative fraction cells, BMMCs from MM aspirates were depleted of CD138 by magnetic beads, as previously described⁶⁶.

Cell culture and 3DTEBM culture. MM cell lines, MM.1S, H929, and OPM2, were purchased from American Type Culture Collection (Rockville, MD). All cell lines were cultured in RPMI-1640 media (Corning, Corning, NY) supplemented with 10% fetal bovine serum, 2 mmol/L L-glutamine, 100 µg/mL penicillin, and 100 µg/mL streptomycin. All cells were cultured at 37 °C and in 5% CO₂ in a NuAire water jacket incubator (Plymouth, MN).

3DTEBM were prepared as previously described⁹. Briefly, cells of interest were plated in 96-well plate in a mixture of BM supernatant, RPMI media, tranexamic acid, and calcium chloride (10 mg/mL). After the 3D matrix cross-links, they were supplemented with media on top and cultured at 37 °C and 5% CO₂. At the end of

the experiment, matrix were digested by type I collagenase, CountBright absolute counting beads (ThermoFisher) were added to each well, and samples were filtered using a 35 μ m nylon mesh filter and subsequently analyzed using flow cytometry (MACSQuant Analyzer 16, Miltenyi Biotec, Bergisch Gladbach, Germany).

Correlation of 2D and 3DTEBM IC₅₀ values with clinical C_{ss} values. The drugs used for the correlation study were carfilzomib, bortezomib, ixazomib, panobinostat, lenalidomide, pomalidomide, dexamethasone, etoposide, doxorubicin, daratumumab, and melphalan for MM. Summary of 2D-Literature, 2D-Experimental, and 3DTEBM IC₅₀ values, as well as clinical C_{ss} values for each drug are shown in Table 1.

The steady state plasma drug concentration (C_{ss}) was determined based on pharmacokinetic data from Phase 1 and/or Phase 2 clinical trials. For 2D-Literature IC₅₀ values, 48 h IC₅₀ values of MM cell lines from at least two studies were averaged. For 2D-Experimental IC₅₀ values, MM cells (MM.1S, H929, and OPM2) were seeded at 50,000 cells per well in 96-well plate and treated with or without incremental concentration for respective drugs for 48 h. Cell survival was determined by MTT assay as previously described⁶⁷. Briefly, MTT solution was added to the cells for 3 h, then the stop solution was added to dissolve the formazan crystals overnight. Wells were read with SpectraMax i3 multimode microplate spectrophotometer (Molecular Devices, San Jose, CA) at 570 nm.

3DTEBM IC₅₀ values were found by increasing the concentration of each drug inside and on top of the 3DTEBM cultures for three different cell lines (MM.1S, H929, and OPM2). 3DTEBM were prepared with DiO-labeled MM cells (50,000/well), BM negative fraction (50,000/well, pooled from 5 RRMM patients), and BM plasma (pooled from 5 RRMM patients), and RPMI media mixed with treatment. After crosslinking of 3DTEBM for 2 h, the matrix was supplemented with 10% plasma in RPMI media on top. Drug treatment was performed at 0.3X, 1X, 3X, and 10X the C_{ss} concentration in the 3DTEBM for 48 h. At the end of the experiment, 3D matrix were digested by collagenase and counting beads were added to each well. Each sample was filtered and analyzed using flow cytometry for the number of the DiO-labeled cancer cells, and normalized to the number of beads. Dose escalation curves were graphed, and the IC₅₀ concentrations for each drug in the three cell lines were determined and averaged to find the final 3DTEBM IC₅₀ values.

Retrospective MM patient 3DTEBM responses. Patient BM samples (unsorted BMNCs and BM plasma) were collected before the start of the clinical treatment regimen. Samples were provided to Cellatrix, along with the treatment regimen that each patient received after the BM biopsy; however, Cellatrix was blinded to the clinical outcomes. Cellatrix treated each patient sample with the corresponding regimen in the 3DTEBM and provided the ex vivo response back to the clinical team (as demonstrated in Fig. 1B).

Patient 3DTEBM were developed by seeding 1×10^5 BMNCs per well with patient's autologous BM plasma and treated with or without the corresponding drug regimen in increasing concentrations (3X and 10X of C_{ss} of individual drugs). Following four days of treatment, cultures were digested to retrieve the cells for flow cytometry analysis. Samples were stained with CD3, CD14, CD16, CD19 and CD123 (all of which were FITC) in addition to CD38 (APC), according to our previously published MM detection method⁶⁸. For flow analysis, live cells were first gated as FSC-hi. Then, MM cell survival was determined by number of FITC-/APC+ cells, normalized to counting beads, and the effect of the drug treatment was calculated as percent of untreated control.

Ex vivo response was analyzed by ANOVA and the responsiveness was provided to the clinical team. The clinical response was determined by the clinical team after a cycle of respective regimen, defined according to the Criteria of the International Myeloma Working Group⁶⁹. The clinical team correlated the ex vivo response with the clinical response for each patient.

Statistical analyses. All patient sample data experiments were expressed as means \pm standard deviation. Sample size was estimated using published guidelines. 3DTEBM experiments were performed in quadruplicates. Residuals were used to analyze data normality, and we examined the expected variance by analyzing the variance similarity across groups. Statistical significance for comparing ex vivo response of primary cells across different concentrations was analyzed using a one-way analysis of variance (ANOVA). P-values < 0.05 were considered statistically significant. Correlation between IC₅₀ and C_{ss} values determined by linear regression fitting.

Data availability

All data generated are available upon request.

Received: 18 May 2021; Accepted: 7 September 2021

Published online: 29 September 2021

References

1. Letai, A. Functional precision cancer medicine—moving beyond pure genomics. *Nat. Med.* **23**, 1028–1035. <https://doi.org/10.1038/nm.4389> (2017).
2. Federico, C. *et al.* Tumor microenvironment-targeted nanoparticles loaded with bortezomib and ROCK inhibitor improve efficacy in multiple myeloma. *Nat. Commun.* **11**, 6037. <https://doi.org/10.1038/s41467-020-19932-1> (2020).
3. Azab, A. K. *et al.* Hypoxia promotes dissemination of multiple myeloma through acquisition of epithelial to mesenchymal transition-like features. *Blood* **119**, 5782–5794. <https://doi.org/10.1182/blood-2011-09-380410> (2012).
4. Azab, A. K. *et al.* The influence of hypoxia on CML trafficking through modulation of CXCR4 and E-cadherin expression. *Leukemia* **27**, 961–964. <https://doi.org/10.1038/leu.2012.353> (2013).
5. Muz, B., de la Puente, P., Azab, F., Ghobrial, I. M. & Azab, A. K. Hypoxia promotes dissemination and colonization in new bone marrow niches in Waldenstrom macroglobulinemia. *Mol. Cancer Res.* **13**, 263–272. <https://doi.org/10.1158/1541-7786.MCR-14-0150> (2015).
6. Muz, B. *et al.* PYK2/FAK inhibitors reverse hypoxia-induced drug resistance in multiple myeloma. *Haematologica* **104**, e310–e313. <https://doi.org/10.3324/haematol.2018.194688> (2019).

7. de la Puente, P. & Azab, A. K. 3D tissue-engineered bone marrow: what does this mean for the treatment of multiple myeloma?. *Fut. Oncol. (Lond., England)* **12**, 1545–1547. <https://doi.org/10.2217/fon-2016-0057> (2016).
8. Weisberg, E. *et al.* Inhibition of CXCR4 in CML cells disrupts their interaction with the bone marrow microenvironment and sensitizes them to nilotinib. *Leukemia* **26**, 985–990. <https://doi.org/10.1038/leu.2011.360> (2012).
9. de la Puente, P. *et al.* 3D tissue-engineered bone marrow as a novel model to study pathophysiology and drug resistance in multiple myeloma. *Biomaterials* **73**, 70–84. <https://doi.org/10.1016/j.biomaterials.2015.09.017> (2015).
10. Sun, J. *et al.* Targeting CD47 as a novel immunotherapy for multiple myeloma. *Cancers (Basel)* **12**, 1. <https://doi.org/10.3390/cancers12020305> (2020).
11. Kinan Alhallak *et al.* 3D Tissue Engineered Plasma Cultures Support Leukemic Proliferation and Induces Drug Resistance. *Leukemia & Lymphoma* (2021).
12. Alhallak, K. *et al.* Nanoparticle T-cell engagers as a modular platform for cancer immunotherapy. *Leukemia* <https://doi.org/10.1038/s41375-021-01127-2> (2021).
13. van de Donk, N. W. C. J., Pawlyn, C. & Yong, K. L. Multiple myeloma. *The Lancet* **397**, 410–427. [https://doi.org/10.1016/s0140-6736\(21\)00135-5](https://doi.org/10.1016/s0140-6736(21)00135-5) (2021).
14. Kumar, S. K. *et al.* Early relapse after autologous hematopoietic cell transplantation remains a poor prognostic factor in multiple myeloma but outcomes have improved over time. *Leukemia* **32**, 986–995. <https://doi.org/10.1038/leu.2017.331> (2017).
15. Bazarbachi, A. H., Al Hamed, R., Malard, F., Harsousseau, J.-L. & Mohty, M. Relapsed refractory multiple myeloma: a comprehensive overview. *Leukemia* **33**, 2343–2357. <https://doi.org/10.1038/s41375-019-0561-2> (2019).
16. Badros, A. Z. *et al.* Carfilzomib in multiple myeloma patients with renal impairment: pharmacokinetics and safety. *Leukemia* **27**, 1707–1714. <https://doi.org/10.1038/leu.2013.29> (2013).
17. Wang, Z. *et al.* Clinical pharmacokinetics, metabolism, and drug-drug interaction of carfilzomib. *Drug Metab. Dispos.* **41**, 230–237. <https://doi.org/10.1124/dmd.112.047662> (2013).
18. Watanabe, T. *et al.* A phase 1/2 study of carfilzomib in Japanese patients with relapsed and/or refractory multiple myeloma. *Br. J. Haematol.* **172**, 745–756. <https://doi.org/10.1111/bjh.13900> (2016).
19. Hurchla, M. A. *et al.* The epoxyketone-based proteasome inhibitors carfilzomib and orally bioavailable oprozomib have anti-resorptive and bone-anabolic activity in addition to anti-myeloma effects. *Leukemia* **27**, 430–440. <https://doi.org/10.1038/leu.2012.183> (2013).
20. Eda, H. *et al.* A novel Bruton's tyrosine kinase inhibitor CC-292 in combination with the proteasome inhibitor carfilzomib impacts the bone microenvironment in a multiple myeloma model with resultant antimyeloma activity. *Leukemia* **28**, 1892–1901. <https://doi.org/10.1038/leu.2014.69> (2014).
21. Hawley, T. S. *et al.* Identification of an ABCB1 (P-glycoprotein)-positive carfilzomib-resistant myeloma subpopulation by the pluripotent stem cell fluorescent dye CDy1. *Am. J. Hematol.* **88**, 265–272. <https://doi.org/10.1002/ajh.23387> (2013).
22. Moreau, P. *et al.* Subcutaneous versus intravenous administration of bortezomib in patients with relapsed multiple myeloma: a randomised, phase 3, non-inferiority study. *Lancet Oncol.* **12**, 431–440. [https://doi.org/10.1016/S1470-2045\(11\)70081-X](https://doi.org/10.1016/S1470-2045(11)70081-X) (2011).
23. Clemens, J. *et al.* Cellular uptake kinetics of bortezomib in relation to efficacy in myeloma cells and the influence of drug transporters. *Cancer Chemother. Pharmacol.* **75**, 281–291. <https://doi.org/10.1007/s00280-014-2643-1> (2015).
24. Garcia-Gomez, A. *et al.* Preclinical activity of the oral proteasome inhibitor MLN9708 in Myeloma bone disease. *Clin. Cancer Res.* **20**, 1542–1554. <https://doi.org/10.1158/1078-0432.CCR-13-1657> (2014).
25. Wong, K. Y., Wan, T. S., So, C. C. & Chim, C. S. Establishment of a bortezomib-resistant Chinese human multiple myeloma cell line: MMLAL. *Cancer Cell Int.* **13**, 122. <https://doi.org/10.1186/1475-2867-13-122> (2013).
26. Gupta, N. *et al.* A pharmacokinetics and safety phase 1/1b study of oral ixazomib in patients with multiple myeloma and severe renal impairment or end-stage renal disease requiring haemodialysis. *Br. J. Haematol.* **174**, 748–759. <https://doi.org/10.1111/bjh.14125> (2016).
27. Richardson, P. G. *et al.* Phase 1 study of twice-weekly ixazomib, an oral proteasome inhibitor, in relapsed/refractory multiple myeloma patients. *Blood* **124**, 1038–1046. <https://doi.org/10.1182/blood-2014-01-548826> (2014).
28. Chauhan, D. *et al.* In vitro and in vivo selective antitumor activity of a novel orally bioavailable proteasome inhibitor MLN9708 against multiple myeloma cells. *Clin. Cancer Res.* **17**, 5311–5321. <https://doi.org/10.1158/1078-0432.CCR-11-0476> (2011).
29. Savelieva, M. *et al.* Population pharmacokinetics of intravenous and oral panobinostat in patients with hematologic and solid tumors. *Eur. J. Clin. Pharmacol.* **71**, 663–672. <https://doi.org/10.1007/s00228-015-1846-7> (2015).
30. Mu, S. *et al.* Panobinostat PK/PD profile in combination with bortezomib and dexamethasone in patients with relapsed and relapsed/refractory multiple myeloma. *Eur. J. Clin. Pharmacol.* **72**, 153–161. <https://doi.org/10.1007/s00228-015-1967-z> (2016).
31. Maiso, P. *et al.* The histone deacetylase inhibitor LBH589 is a potent antimyeloma agent that overcomes drug resistance. *Cancer Res.* **66**, 5781–5789. <https://doi.org/10.1158/0008-5472.CAN-05-4186> (2006).
32. Catley, L. *et al.* Aggresome induction by proteasome inhibitor bortezomib and alpha-tubulin hyperacetylation by tubulin deacetylase (TDAC) inhibitor LBH589 are synergistic in myeloma cells. *Blood* **108**, 3441–3449. <https://doi.org/10.1182/blood-2006-04-016055> (2006).
33. Hofmeister, C. C. *et al.* Phase I trial of lenalidomide and CCI-779 in patients with relapsed multiple myeloma: evidence for lenalidomide-CCI-779 interaction via P-glycoprotein. *J. Clin. Oncol.* **29**, 3427–3434. <https://doi.org/10.1200/JCO.2010.32.4962> (2011).
34. Hou, J. *et al.* A multicenter, open-label, phase 2 study of lenalidomide plus low-dose dexamethasone in Chinese patients with relapsed/refractory multiple myeloma: the MM-021 trial. *J. Hematol. Oncol.* **6**, 41. <https://doi.org/10.1186/1756-8722-6-41> (2013).
35. Richardson, P. G. *et al.* Immunomodulatory drug CC-5013 overcomes drug resistance and is well tolerated in patients with relapsed multiple myeloma. *Blood* **100**, 3063–3067. <https://doi.org/10.1182/blood-2002-03-0996> (2002).
36. Xu, Q. *et al.* Expression of the cereblon binding protein argonaute 2 plays an important role for multiple myeloma cell growth and survival. *BMC Cancer* **16**, 297. <https://doi.org/10.1186/s12885-016-2331-0> (2016).
37. Greenberg, A. J., Walters, D. K., Kumar, S. K., Rajkumar, S. V. & Jelinek, D. F. Responsiveness of cytogenetically discrete human myeloma cell lines to lenalidomide: lack of correlation with cereblon and interferon regulatory factor 4 expression levels. *Eur. J. Haematol.* **91**, 504–513. <https://doi.org/10.1111/ejh.12192> (2013).
38. Matsue, K. *et al.* Pomalidomide alone or in combination with dexamethasone in Japanese patients with refractory or relapsed and refractory multiple myeloma. *Cancer Sci.* **106**, 1561–1567. <https://doi.org/10.1111/cas.12772> (2015).
39. Rychak, E. *et al.* Pomalidomide in combination with dexamethasone results in synergistic anti-tumour responses in pre-clinical models of lenalidomide-resistant multiple myeloma. *Br. J. Haematol.* **172**, 889–901. <https://doi.org/10.1111/bjh.13905> (2016).
40. Guglielmelli, T. *et al.* mTOR pathway activation in multiple myeloma cell lines and primary tumour cells: pomalidomide enhances cytoplasmic-nuclear shuttling of mTOR protein. *Oncoscience* **2**, 382–394. <https://doi.org/10.18632/oncoscience.148> (2015).
41. Iida, S. *et al.* Lenalidomide plus dexamethasone treatment in Japanese patients with relapsed/refractory multiple myeloma. *Int. J. Hematol.* **92**, 118–126. <https://doi.org/10.1007/s12185-010-0624-7> (2010).
42. Mao, X. *et al.* A chemical biology screen identifies glucocorticoids that regulate c-maf expression by increasing its proteasomal degradation through up-regulation of ubiquitin. *Blood* **110**, 4047–4054. <https://doi.org/10.1182/blood-2007-05-088666> (2007).
43. Stewart, H. J., Kishikova, L., Powell, F. L., Wheatley, S. P. & Chevassut, T. J. The polo-like kinase inhibitor BI 2536 exhibits potent activity against malignant plasma cells and represents a novel therapy in multiple myeloma. *Exp. Hematol.* **39**, 330–338. <https://doi.org/10.1016/j.exphem.2010.12.006> (2011).

44. Chen, Y. H. *et al.* Inhibition of myeloma cell growth by dexamethasone and all-trans retinoic acid: synergy through modulation of interleukin-6 autocrine loop at multiple sites. *Blood* **87**, 314–323 (1996).
45. Friday, E., Ledet, J. & Turturro, E. Response to dexamethasone is glucose-sensitive in multiple myeloma cell lines. *J. Exp. Clin. Cancer Res.* **30**, 81. <https://doi.org/10.1186/1756-9966-30-81> (2011).
46. Dorr, R. T. *et al.* Comparative pharmacokinetic study of high-dose etoposide and etoposide phosphate in patients with lymphoid malignancy receiving autologous stem cell transplantation. *Bone Marrow Transpl.* **31**, 643–649. <https://doi.org/10.1038/sj.bmt.1703906> (2003).
47. Osby, E., Liliemark, E., Bjorkholm, M. & Liliemark, J. Oral etoposide in patients with hematological malignancies: a clinical and pharmacokinetic study. *Med. Oncol.* **18**, 269–275. <https://doi.org/10.1385/MO:18:4:269> (2001).
48. Dvorakova, K. *et al.* Molecular and cellular characterization of imexon-resistant RPMI8226/I myeloma cells. *Mol Cancer Ther.* **1**, 185–195 (2002).
49. Dimberg, L. Y. *et al.* Stat1 activation attenuates IL-6 induced Stat3 activity but does not alter apoptosis sensitivity in multiple myeloma. *BMC Cancer* **12**, 318. <https://doi.org/10.1186/1471-2407-12-318> (2012).
50. Demel, H. R. *et al.* Effects of topoisomerase inhibitors that induce DNA damage response on glucose metabolism and PI3K/Akt/mTOR signaling in multiple myeloma cells. *Am. J. Cancer Res.* **5**, 1649–1664 (2015).
51. Orłowski, R. Z. *et al.* Phase 1 trial of the proteasome inhibitor bortezomib and pegylated liposomal doxorubicin in patients with advanced hematologic malignancies. *Blood* **105**, 3058–3065. <https://doi.org/10.1182/blood-2004-07-2911> (2005).
52. Shushanov, S. S. & Kravtsova, T. A. Cytotoxic effect of doxorubicin on human multiple myeloma cells in vitro. *Bull. Exp. Biol. Med.* **155**, 228–232. <https://doi.org/10.1007/s10517-013-2120-6> (2013).
53. Zhang, H., Chen, J., Zeng, Z., Que, W. & Zhou, L. Knockdown of DEPTOR induces apoptosis, increases chemosensitivity to doxorubicin and suppresses autophagy in RPMI-8226 human multiple myeloma cells in vitro. *Int. J. Mol. Med.* **31**, 1127–1134. <https://doi.org/10.3892/ijmm.2013.1299> (2013).
54. Saha, M. N., Chen, Y., Chen, M. H., Chen, G. & Chang, H. Small molecule MIRA-1 induces in vitro and in vivo anti-myeloma activity and synergizes with current anti-myeloma agents. *Br. J. Cancer* **110**, 2224–2231. <https://doi.org/10.1038/bjc.2014.164> (2014).
55. Egerer, G. *et al.* The NK(1) receptor antagonist aprepitant does not alter the pharmacokinetics of high-dose melphalan chemotherapy in patients with multiple myeloma. *Br. J. Clin. Pharmacol.* **70**, 903–907. <https://doi.org/10.1111/j.1365-2125.2010.03792.x> (2010).
56. Osterborg, A., Ehrsson, H., Eksborg, S., Wallin, I. & Mellstedt, H. Pharmacokinetics of oral melphalan in relation to renal function in multiple myeloma patients. *Eur. J. Cancer Clin. Oncol.* **25**, 899–903. [https://doi.org/10.1016/0277-5379\(89\)90138-7](https://doi.org/10.1016/0277-5379(89)90138-7) (1989).
57. Ray, A. *et al.* A novel alkylating agent Melflufen induces irreversible DNA damage and cytotoxicity in multiple myeloma cells. *Br. J. Haematol.* **174**, 397–409. <https://doi.org/10.1111/bjh.14065> (2016).
58. Cukrova, V., Neuwirtova, R., Cermak, J. & Neuwirt, J. Inhibitor of normal granulopoiesis produced by cells of MDS patients. *Neoplasma* **36**, 83–89 (1989).
59. Mandl-Weber, S. *et al.* The novel inhibitor of histone deacetylase resminostat (RAS2410) inhibits proliferation and induces apoptosis in multiple myeloma (MM) cells. *Br. J. Haematol.* **149**, 518–528. <https://doi.org/10.1111/j.1365-2141.2010.08124.x> (2010).
60. Harrison, R. K. Phase II and phase III failures: 2013–2015. *Nat. Rev. Drug Discov.* **15**, 817–818. <https://doi.org/10.1038/nrd.2016.184> (2016).
61. Silva, A. *et al.* An Ex Vivo Platform for the Prediction of Clinical Response in Multiple Myeloma. *Cancer Res.* **77**, 3336–3351. <https://doi.org/10.1158/0008-5472.CAN-17-0502> (2017).
62. Papadimitriou, K. *et al.* Ex Vivo Models Simulating the Bone Marrow Environment and Predicting Response to Therapy in Multiple Myeloma. *Cancers (Basel)* **12**, <https://doi.org/10.3390/cancers12082006> (2020).
63. Sudalagunta, P. *et al.* A pharmacodynamic model of clinical synergy in multiple myeloma. *EBioMedicine* **54**, 102716. <https://doi.org/10.1016/j.ebiom.2020.102716> (2020).
64. Walker, Z. J. *et al.* Measurement of ex vivo resistance to proteasome inhibitors, IMiDs, and daratumumab during multiple myeloma progression. *Blood Adv.* **4**, 1628–1639. <https://doi.org/10.1182/bloodadvances.2019000122> (2020).
65. Muz, B. *et al.* CXCR4-targeted PET imaging using (64)Cu-AMD3100 for detection of Waldenström Macroglobulinemia. *Cancer Biol. Ther.* **21**, 52–60. <https://doi.org/10.1080/15384047.2019.1665405> (2020).
66. de la Puente, P. *et al.* Enhancing proteasome-inhibitory activity and specificity of bortezomib by CD38 targeted nanoparticles in multiple myeloma. *J. Control. Release* **270**, 158–176. <https://doi.org/10.1016/j.jconrel.2017.11.045> (2018).
67. Federico, C. *et al.* Localized Delivery of Cisplatin to Cervical Cancer Improves Its Therapeutic Efficacy and Minimizes Its Side Effect Profile. *Int. J. Radiat. Oncol. Biol. Phys.* **109**, 1483–1494. <https://doi.org/10.1016/j.ijrobp.2020.11.052> (2021).
68. Muz, B. *et al.* A CD138-independent strategy to detect minimal residual disease and circulating tumour cells in multiple myeloma. *Br. J. Haematol.* **173**, 70–81. <https://doi.org/10.1111/bjh.13927> (2016).
69. Rajkumar, S. V. *et al.* International Myeloma Working Group updated criteria for the diagnosis of multiple myeloma. *Lancet Oncol.* **15**, e538–548. [https://doi.org/10.1016/S1470-2045\(14\)70442-5](https://doi.org/10.1016/S1470-2045(14)70442-5) (2014).

Acknowledgements

This study was supported by the Paula C. and Rodger O. Riney Blood Cancer Research Initiative Fund. K.A. was funded by an award from the National Center for Advancing Translational Sciences of the National Institutes of Health (TL1TR002344).

Author contributions

P.P. and A.J. conducted experiments and analyzed data. K.A. conducted experiments, analyzed data and wrote the manuscript. J.S. analyzed data and wrote the manuscript. M.F. provided clinical samples and analyzed data. F.A., B.M., and I.S. analyzed data. R.V. designed experiments, provided clinical samples and analyzed data. J.F.D. designed experiments, A.K.A. conceived the idea, designed experiments, analyzed the data and wrote the manuscript. All authors reviewed and approved the manuscript.

Competing interests

A.K.A. and P.P. have patents describing the 3DTBM technology used in this study, and are the founders and owners of Cellatrix LLC. F.A. is an employee of Cellatrix LLC. A.J. was an employee of Cellatrix LLC. Other authors state no conflicts of interest.

Additional information

Supplementary Information The online version contains supplementary material available at <https://doi.org/10.1038/s41598-021-98760-9>.

Correspondence and requests for materials should be addressed to A.K.A.

Reprints and permissions information is available at www.nature.com/reprints.

Publisher's note Springer Nature remains neutral with regard to jurisdictional claims in published maps and institutional affiliations.



Open Access This article is licensed under a Creative Commons Attribution 4.0 International License, which permits use, sharing, adaptation, distribution and reproduction in any medium or format, as long as you give appropriate credit to the original author(s) and the source, provide a link to the Creative Commons licence, and indicate if changes were made. The images or other third party material in this article are included in the article's Creative Commons licence, unless indicated otherwise in a credit line to the material. If material is not included in the article's Creative Commons licence and your intended use is not permitted by statutory regulation or exceeds the permitted use, you will need to obtain permission directly from the copyright holder. To view a copy of this licence, visit <http://creativecommons.org/licenses/by/4.0/>.

© The Author(s) 2021